Carbohydrate Research 415 (2015) 12–16

Contents lists available at ScienceDirect

Carbohydrate Research

journal homepage: www.elsevier.com/locate/carres

# Stereoselective synthesis and molecular modeling of chiral cyclopentanes

Raid J. Abdel-Jalil [a,*], Thomas Steinbrecher [b], Thuraya Al-Harthy [a], Ahmed Mahal [c], Osama K. Abou-Zied [a], Wolfgang Voelter [d]

[a] Chemistry Department, College of Science, Sultan Qaboos University, Muscat, Oman
[b] Abteilung für Theoretische Chemische Biologie, Institut für Physikalische Chemie, Karlsruher Institut für Technologie, D-76131 Karlsruhe, Germany
[c] Department of Chemistry of the Natural Products, University of Naples Federico II, Napoli, Campania, Italy
[d] IFIB – Interfakultäres Institut für Biochemie, University of Tuebingen, Tuebingen, Germany

ARTICLE INFO

*Article history:*
Received 21 May 2015
Received in revised form 22 June 2015
Accepted 1 July 2015
Available online 23 July 2015

*Keywords:*
Asymmetric synthesis
Cyclopentane
Molecular modeling
Molecular dynamics

ABSTRACT

The reaction of 3-methyseleno-2-methylselenomethyl-propene with benzyl 2,3-anhydro-4-*O*-triflyl-β-L-ribopyranoside provides a major convenient enantiomeric product of 1-methylene-(benzyl3, 4-dideoxy-α-D-arabinopyranoso)-[3,4-c]-cyclopentane, with benzyl-2,3-anhydro-4-deoxy-4-*C*-(2-methyl- propen-3-yl)-α-D-lyxopyranoside as a minor product. While the reaction of 3-methyseleno-2-[methylselenomethyl]-propene with benzyl 2,3-anhydro-4-*O*-triflyl-α-D-ribopyranoside produces a good yield of benzyl-2,3-anhydro-4-deoxy-4-*C*-(2-methylpropen-3-yl)-α-D-lyxo-pyranoside. Molecular modeling and molecular dynamics simulations indicate that the intermediate in the reaction of the β-L sugar frequently occupies an optimal conformation that leads to the formation of cyclopentane, while the intermediate in the reaction of the α-D sugar has a very small probability. The results point to the dominant role of the β-L sugar intermediate in controlling the cyclopentane formation.



## 1. Introduction

The construction of asymmetric cyclopentanemoieties has received much attention in recent years due to their diversity and frequency of multifunctional five-membered carbocyclic structures in natural products and their interesting biological activities.[1–3] Moreover, the significance of the development of new synthetic strategies leading to construct such diverse complex molecular structures arises due to their essential need in total synthesis of natural products and the high demand for synthetic strategies, which can provide alternative and practical methods for the synthesis of pharmaceuticals and agrochemicals. Pactamycin (**1**) and pactamycin derivative (**2**) have been shown to possess antitumor and antibacterial activities[4] whereas CCR5 (**3**) has been reported as an anti-HIV drug candidate.[5] Viridenomycin (**4**) have shown potent antimicrobial activities[6] against Gram positive and negative organisms (Fig. 1).

Although, many methods for the construction of cyclopentane rings onto preexisting cyclic compounds are reviewed,[7–11] one of the most straightforward methods, the annelation of a cyclopentane ring on a pyranoside nucleus has not been reported, to the best of our knowledge. In the present work, we describe a one-step regio- and stereo-selective annelation of highly functionalized cyclopentane on pyranoside ring.

We have previously reported several methods for the asymmetric synthesis of heterocyclic systems; e.g. piperazines,[12] morpholines,[13] cyclic trithiocarbonates[14] and thiazolidines[15] using carbohydrates as chiral scaffolds. Our basic strategy involves stereospecific nucleophilic substitution of the triflate group followed by intramolecular nucleophilic opening of the adjacent epoxy group. In continuation of our efforts on the development of novel synthetic strategies for asymmetric construction of complex molecular structures, we utilized the reaction of 3-methyseleno-2-[methylselenomethyl]-propene[16] (**5**, Scheme 1), as a valuable reagent, able to transfer a four carbon unit to various derivatives with the β-L-anhydro triflate **6** and its α-D isomer **7**.

## 2. Results and discussion

### 2.1. Synthesis

The synthesis of β-L-anhydro triflate **6** was successfully achieved in six steps,[17] starting from the commercially available L-arabinose and following a multi-step synthetic strategy including benzylation, selective protection, tosylation, deprotection, intramolecular $S_N2$ reaction, and triflation. On the other hand, the synthesis of the α-D-isomer **9** was prepared in eight steps following an alternative procedure[18] which includes benzoylation, $S_N2$ reaction, deprotection,

* Corresponding author. Chemistry Department, College of Science, Sultan Qaboos University, Muscat 123, Oman. Tel.: + 96892089702; fax: +968 24413391.
*E-mail address:* jalil@squ.edu.om (R.J. Abdel-Jalil).

http://dx.doi.org/10.1016/j.carres.2015.07.012
0008-6215/

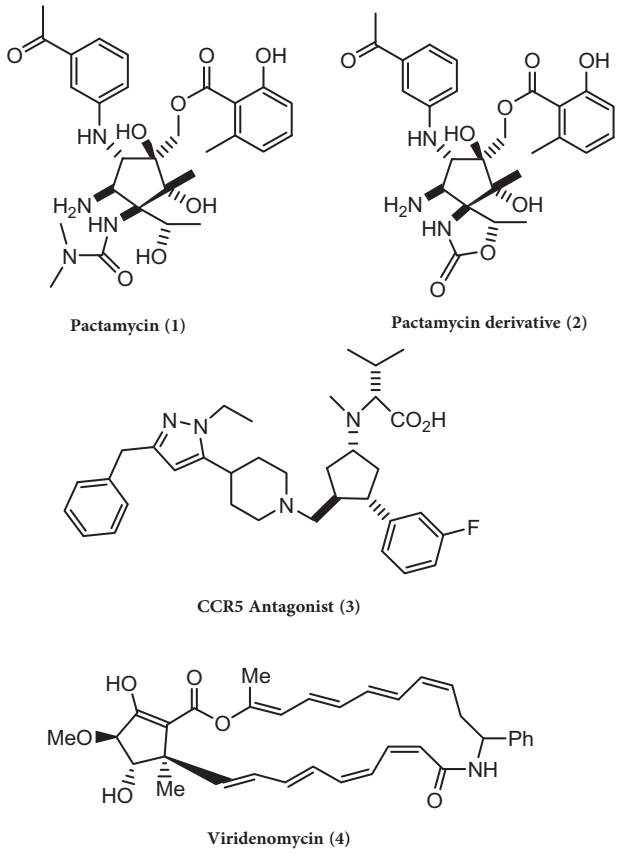


**Fig. 1.** Representative structures of cyclopentane-containing natural products.

intramolecular $S_N2$ reaction, and triflation. The reaction of the intermediary reagent 3-lithio-2-[lithiomethyl]-propene (formed from the sequential addition of two equivalents of *sec*-BuLi to **5** in THF at –78 °C) with the sugar triflate **6** at the same temperature leads to the formation of 1-methylene-(benzyl3,4-dideoxy-α-D-arabino-pyranoso)-[3,4-c]- cyclopentane (**8**) and benzyl-2,3-anhydro-4-deoxy-4-*C*-(2-methyl-propen-3-yl)-α-D-lyxo-pyranoside (**7**), in 77 and 5% yield, respectively (Scheme 1).

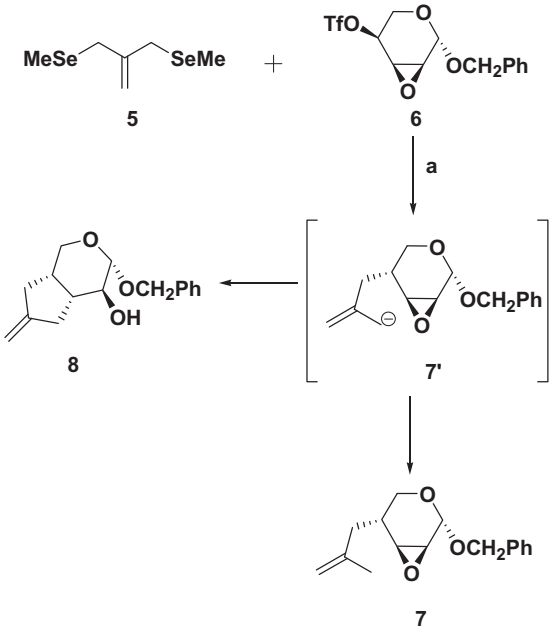


**Scheme 1.** Synthesis of **7** and **8** (a) *sec*-BuLi, THF, –78 °C.

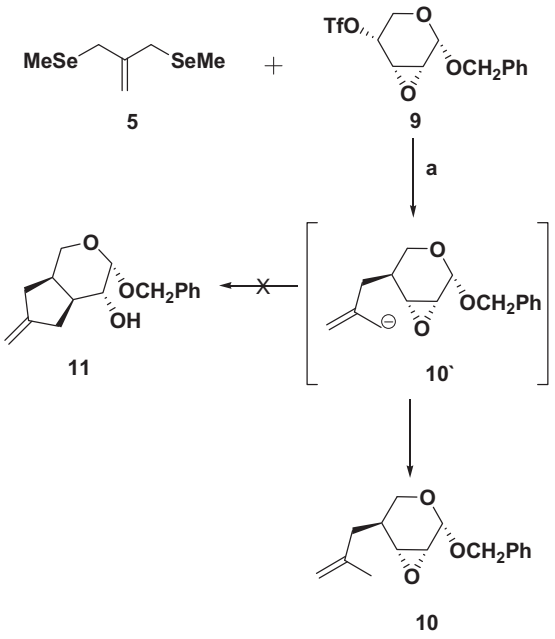


**Scheme 2.** Synthesis of **10** and **11** (a) sec-BuLi, THF, –78 °C.

Surprisingly when the same reaction conditions were applied to the α-D-anhydro triflate isomer **9**, the major product was the non-cyclized product **10** in 60% yield and there were no traces for the formation of the expected cyclopentane derivative **11** as shown in Scheme 2. We tried several reaction conditions, but did not detect any traces of **11**. These included changing the equivalents of sec-BuLi (one to five equivalents), changing the solvent of the reaction (diethylether) and changing the temperature of the reaction (from –78 °C to room temperature), after the formation of the carbanion intermediate at –78 °C.

Despite all attempts to vary the reaction conditions, the major product in the reaction of α-D- isomer **9** is always the non-cyclized compound **10**. The combined use of 2D homo- and hetero-nuclear chemical shift correlation spectroscopy allowed the unambiguous and complete assignment of the proton and carbon chemical shifts of the new cyclopentane derivative **8**. Thus, in the $^1$H NMR spectrum of **8**, H-1 appears as a doublet with (J = 4.3 Hz) at δ = 4.27 ppm, representing diequatorial relationship with H-2. The predominant conformation is therefore $^4C_1$. Successful transformation of the sugar triflate **6** into the cyclopentane derivative **8** is manifested in the disappearance of the two oxirane ring peaks in the $^{13}$C NMR spectrum (normally appear at around 50–52 ppm in the sugar triflate **6**) and the appearance of two upfield peaks at δ = 39.4 and 43.5 ppm, correlated to C-3 and C-4, respectively. In the $^{13}$C NMR spectrum of **7**, the two oxirane ring peaks resonate at δ = 50.1 and 54.2 ppm and the appearance of a singlet methyl peak at δ = 1.75 ppm in the $^1$H NMR spectrum prove the proposed structure of this minor product.

### 2.2. Theoretical modeling

We obtained average heats of formation ($\Delta H^0_f$) for the four compounds at 298 K from 10 ns of semiempirical QM molecular dynamics data (Table 1). The expected two reaction products **8** and **11** are found to have very similar heats of formation, to within the calculation uncertainty. In contrast, the reaction intermediates **7′** and **10′** exhibit different $\Delta H^0_f$ values. **7′**, the intermediate through

**Table 1**
Calculated heat of formation for the prepared compounds

| Compound | Net charge | $\Delta H^0_f$ [kcal/mol] |
|---|---|---|
| **7′** | −1 | −16.5 ± 0.4 |
| **10′** | −1 | −13.3 ± 0.2 |
| **8** | 0 | −38.5 ± 0.2 |
| **11** | 0 | −38.4 ± 0.2 |

which the reaction is known to proceed was found to be 3.2 kcal/mol enthalpically more stable than **10′**. Error estimates from batch averaging over 1 ns trajectory subsets show the difference to be significantly above the expected margin of error. We have analyzed the conformational ensembles of **7′** and **10′** to determine the structural reasons underlying their different stabilities.

Conformational fluctuations over 10 ns trajectory lengths were similar for all four compounds, with all-atom rmsd-values of ca. 2.4 ± 0.4 Å in all cases (data not shown). For a more detailed look at the structures, we have defined five geometrical parameters, the three dihedral angles α, β and γ, the distance d and the angle δ.

Dihedral α measures the orientation of the sec-butyl group with respect to the neighboring epoxide carbon ring atom. If it occupies the trans (α ca. 180°) or one of the gauche (α ca. 60°) conformation, the carboanion points away from the tetrahydropyran ring. In the second gauche (α ca. 300°) conformation, the sec-butyl group lies perpendicular to the tetrahydropyran ring, with the carboanion close to its future point of attack at the epoxide carbon atom. For **7′**, the second gauche conformation is observed frequently (in 36% of MD snapshots), while it rarely occurs in **10′** (in 14% of MD snapshots). This influences the average distance d between the carboanion and epoxide carbon only slightly (3.39 Å in **7′** and 3.48 Å in **10′**), but very small values of d below 3 Å, effectively moving the carboanion along the reaction pathway for the epoxide ring opening, are observed more frequently in **7′** than in **10′** (5% and 2.7% of MD snapshots respectively). This indicates that intermediate **7′** frequently occupies an optimal conformation for the following cyclopentane formation reaction, while **10′** does so more rarely.

The tetrahydropyran ring is fairly rigid due to the epoxide ring. It occupies mainly two different conformations, measured by the dihedral β, in all four molecules. We label these conformations 'twist1' (β > 0) and 'twist2' (β < 0). In the 'twist1' conformation, the ring oxygen and epoxide oxygen lie on the same side of the six-membered ring, in the 'twist2' conformation on opposite sides. In the reaction products, the fused cyclopentane ring results in favoring the 'twist1' conformation (in 93% and 69% of MD snapshots for **8** and **11**, respectively). In the reaction intermediates, **7′** favors the 'twist1' conformation, but **10′** does not (found in 68% and 41% of MD snapshots, respectively). Therefore, the **7′** intermediate is more likely to occupy a ring conformation close to the final reaction product than **10′**.

The dihedral angle γ describes the orientation of the benzyl residue with respect to the ring oxygen. For **7′** a strong preference for a gauche-like conformation is found (γ ca. 280°, in 71% of MD snapshots) in which the benzyl group lies perpendicular to the tetrahydropyran ring opposite of the epoxide functionality (Fig. 2). No clear preference for γ is found for **10′**. In the final products, γ is found to predominantly cluster around 120° for **8** and 240° for **11**. Due to the different chiralities, both conformations result in the benzyl residue pointing away from the fused rings.

QM molecular dynamics simulation provides additional insights into the molecular structure underlying the observed reaction pathways. We find one of the reaction intermediates, **7′**, to be more stable than the diastereomeric **10′**. A conformational analysis shows that the different chiralities allow a bent conformation

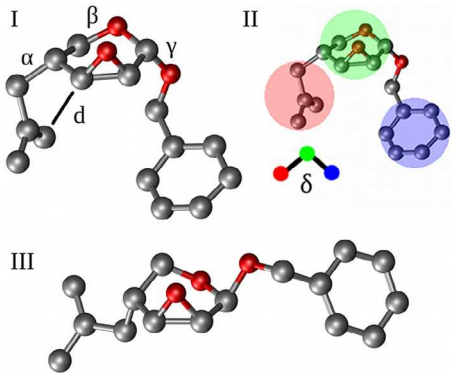


**Fig. 2.** Typical structures of the reaction intermediate products and definition of geometrical parameters. Hydrogen atoms are omitted for clarity. (I) Typical MD structural snapshot of **7′**. Both the sec-butyl and benzyl group lie on the same side of the tetrahydropyran ring, opposite of the epoxide functionality. The ring oxygen occupies the 'twist1' conformation. The three dihedral angles α, β and γ and distance d are indicated. (II) Definition of the angle δ, between the center of mass of the sec-butyl group, tetrahydropyran ring and phenyl residue. (III) Typical structural snapshot of II. The sec-butyl and benzyl group point away from the tetrahydropyran ring. The ring oxygen occupies the 'twist2' conformation.

in which the carboanion is stabilized by the nearby phenyl group in **7′** only. While no reaction rates or barriers can be inferred from the simulations, we could identify unequal stabilization of the reaction intermediates as the reason why product **8** is readily formed and **11** is not.

Our use of a semiempirical quantum mechanics description renders our results free of some of the approximations in classical force fields, e.g. accounting for electronic polarization effects and avoids the need to determine empirical parameters for novel compounds. Due to the moderate computational cost of such calculations, we therefore believe that QM MD simulations of small organic molecules can serve as useful tools for organic chemists. While semiempirical QM models like PM3 do contain significant parameterization, they offer at least a simplified electronic structure model of the system and unlike molecular mechanics models allow for e.g. electronic polarization effects.

## 3. Conclusion

In this work, we tested a new methodology toward stereoselective synthesis of chiral cyclopentane based on the reaction of 2,3-anhydropentose as chiron with 3-methyseleno-2-methylselenomethyl-propene. Theoretical modeling provided evidence for the formation of benzyl-2,3-anhydro-4-deoxy-4-*C*-(2-methyl-propen-3-yl)-α-D-lyxopyranoside. We find that **7′** is more likely to adopt a product like conformations than **10′**. In **7′**, the benzyl and sec-butyl group typically lie close to each other and perpendicular to the six-membered ring, leading to possible stabilization of the carboanion.

## 4. Experimental and theoretical methods

### 4.1. General

All solvents were dried by standard methods and all reactions were carried out under inert atmosphere (argon). Deuterated solvents were used for the $^1$H and $^{13}$C NMR measurements. Mass spectrometric data (MS) were obtained by fast atom bombardment (FAB–MS). For the preparative scale chromatography, silica gel (60–100 mesh) was used.

### 4.2. Synthesis

#### 4.2.1. Synthesis of 3-methylseleno-2-methyl-selenomethyl-1-propene (**5**)

The selenium reagent has been synthesized following literature procedure.[16] Yellow oil; yield: 75%; $^1$H NMR (250 MHz, $CDCl_3$): δ = 1.90 (s, 6H, Se$\underline{CH_3}$, Se′$\underline{CH_3}$), 3.33 (s, 4H, $\underline{CH_2}$Se$\underline{CH_3}$, $\underline{CH_2}$′Se$\underline{CH_3}$), 4.88 (s, 2H, $\underline{CH_2}$═C). GASPE NMR (63 MHz, $CDCl_3$): δ = 4.4 (Se$CH_3$, Se′$CH_3$), 28.8 ($CH_2$SeCH$_3$, $CH_2$′SeCH$_3$), 113.9 ($CH_2$═C), 141.7 (CH$_2$═*C*).

#### 4.2.2. The reaction of β-L-anhydro triflate 6 with 3-methyseleno-2-[methylselenomethyl]-propene (**5**)

A total of 266 mg, 1 mmol, of 3-methyseleno-2-[methylselenomethyl]-propene (**5**) in 20 mL THF was cooled under argon to –78 °C. A solution of *sec*-butyllithium (0.92 mL, 1.2 mmol, 1.3 M in cyclohexane) was slowly added over a period of 10 min. After stirring for 1 h, another 0.92 mL of *sec*-butyllithium was added and the reaction mixture was stirred for an additional hour. A solution of sugar triflate **6** (354 mg, 1 mmol) in 5 mL THF was slowly added and the stirring was continued for another 8 h at –78 °C, whereby the TLC showed no starting material. The reaction was quenched with a saturated $NH_4Cl$ solution (5 mL) and extracted with EtOAc (3 × 30 mL). The combined organic layers were dried over $Na_2SO_4$ and concentrated under reduced pressure to afford a yellow oil which showed two spots on TLC in $CH_2Cl_2$ ($R_f$ = 0.4 as a major product and $R_f$ = 0.82 as a minor product). The mixture was purified by column chromatography to yield **7** and **8**.

*4.2.2.1. Benzyl-2,3-anhydro-4-deoxy-4-*C*-(2-methylpropen-3-yl)-α-D-lyxopyranoside (**7**).* Yellow oil; 13 mg (5% yield); $^1$H NMR (250 MHz, $CDCl_3$): δ = 7.25–7.38 (m, 5H, $C_6H_5$), 5.05 (s, 1H, H-1), 4.83 (bs, 2H, C═$\underline{CH_2}$), 4.79 (d, J = 11.9 Hz, 1H, OC*H*HPh), 4.55 (d, J = 11.9 Hz, 1H, OCH*H*Ph), 3.41 (d, J = 9.01 Hz, 1H, H-5), 3.40 (d, J = 8.0 Hz, 1H, H-5′), 3.12, 3.05 (d, J = 3.9, 3.7 Hz, 1H, 1H, H-2, H-3), 2.29 (m, 1H, H-4), 2.05 (m, 2H, —$CH_2$), 1.75 (s, 3H, $\underline{CH_3}$—C($CH_2$)═$CH_2$). GASPE NMR (250 MHz, $CDCl_3$): δ = 22.2 (C-4), 30.4 ($\underline{C}H_3$—C($CH_2$)═$CH_2$), 38.1 ($CH_3$—C($\underline{C}H_2$)═$CH_2$), 50.1, 54.2 (C-2, C-3), 59.8 (C-5), 69.9 (O$CH_2$Ph), 94.3 (C-1), 112.9 (C═$CH_2$), 128.0–128.6, 137.4 ($C_6H_5$), 141.6 (*C*═$CH_2$). FAB–MS: m/z (%): 261 [M$^+$ + 1]; calculated for $C_{16}H_{20}O_3$: 260.33. Anal. calcd for $C_{16}H_{20}O_3$ (260.33): C, 73.81; H, 7.75. Found: C, 73.59; H, 7.62.

*4.2.2.2. 1-Methylene-(benzyl 3,4-dideoxy-α-D-arab-inopyranoso)-[3,4-c]cyclopentane (**8**).* White solid; m.p. 118–119 °C; 0.201 g (77% yield); $[\alpha]^{20}_D$ = +35.9° (c = 0.20, $CH_2Cl_2$); $^1$H NMR (400 MHz, $CDCl_3$): δ = 7.27–7.34 (m, 5H, $C_6H_5$), 4.92 (bs, 2H, C═$\underline{CH_2}$), 4.88 (d, J = 11.7 Hz, 1H, OC*H*HPh), 4.55 (d, J = 11.7 Hz, 1H, OCH*H*Ph), 4.27 (d, J = 4.3 Hz, 1H, H-1), 3.86 (dd, J = 2.2, 12.1 Hz, 1H, H-5), 3.71 (dd, J = 3.6, 12.1 Hz, 1H, H-5′), 3.28 (ddd, J = 2.2, 7.2, 9.4 Hz, 1H, H-2), 2.61, 2.33–2.47 (ddd, m, J = 1.8, 3.1, 17.1 Hz, 1H, 3H, $C_6$—H, $C_8$-H), 2.21 (m, 1H, H-4), 2.22 (d, J = 2.7 Hz, 1H, O-H), 2.05 (m, 1H, H-3). GASPE NMR (100 MHz, $CDCl_3$): δ = 33.9, 36.8 (C-6, C-8), 39.4 (C-3), 43.5 (C-4), 65.1 (C-5), 70.0 (C-2), 70.4 (O$CH_2$Ph), 103.4 (C-1), 107.5 (C═*C*$H_2$), 127.8–128.0, 137.0 ($C_6H_5$), 149.9 (*C*═$CH_2$). FAB–MS: m/z (%): 261 [M$^+$ + 1]; calculated for $C_{16}H_{20}O_3$: 260.33. Anal. calcd for $C_{16}H_{20}O_3$ (260.33): C, 73.81; H, 7.75. Found: C, 73.66; H, 7.64.

#### 4.2.3. The reaction of α-D-anhydro triflate **9** with 3-methyseleno-2-[methylselenomethyl]-propene (**5**)

The reaction of α-D-anhydro triflate **9** with 3-methyseleno-2-[methylselenomethyl]-propene (**5**) was carried out following the same reaction conditions described above to yield exclusively the non-cyclized product (**10**).

*4.2.3.1. Benzyl-2,3-anhydro-4-deoxy-4-*C*-(2-methylpropen-3-yl)-β-L-lyxopyranoside (9).* Yellow oil; 0.301 g (78% yield); $^1$H NMR (250 MHz, $CDCl_3$): δ = 7.29–7.40 (m, 5H, $C_6H_5$), 5.01 (d, J = 2.4 Hz, 1H, H-1), 4.87 (bs, 2H, C═$\underline{CH_2}$), 4.79 (d, J = 12.2 Hz, 1H, OC*H*HPh), 4.60 (d, J = 12.6 Hz, 1H, OCH*H*Ph), 3.86 (dd, J = 3.4, 12.5 Hz, 1H, H-5), 3.66 (d, J = 12.8 Hz, 1H, H-5′) 3.34 (m, 2H, H-2, H-3), 2.33 (m, 1H, H-4), 2.12 (m, 2H, —$CH_2$), 1.71 (s, 3H, $\underline{CH_3}$—C($CH_2$)═$CH_2$). GASPE NMR (250 MHz, $CDCl_3$): δ = 21.2 (C-4), 31.2 ($\underline{C}H_3$—C($CH_2$)═$CH_2$), 38.5 ($CH_3$—C($\underline{C}H_2$)═$CH_2$) 51.1, 51.8 (C-2, C-3), 57.0 (C-5), 69.1 (O$CH_2$Ph), 92.4 (C-1), 127.8–128.5, 137.6 ($C_6H_5$). FAB–MS: m/z (%): 261 [M$^+$ + 1]; calculated for $C_{16}H_{20}O_3$: 260.33. Anal. calcd for $C_{16}H_{20}O_3$ (260.33): C, 73.81; H, 7.75. Found: C, 73.70; H, 7.82.

### 4.3. Theoretical modeling

All simulations were conducted using the quantum mechanical MD module[19] in version 11 of the *Amber* MD package.[20] The four studied compounds **7′**, **10′**, **8** and **11** were sketched by hand and transformed into 3D-structures. The semiempirical PM3 Hamiltonian[21] combined with a Generalized Born implicit solvent model[22–24] was used as potential function. Using implicit solvation clearly introduces approximations due to the continuum nature of the solvent model. We have chosen the GB solvation model over the alternative of a QM/MM model with explicit solvation primarily for sake of computational efficiency and to avoid adding a QM/MM boundary into the system. In addition, for explicit solvation models of organic solvents reliable parameters are less well established than for water models. The employed implicit solvent model of THF therefore appears to be an efficient solution. An external dielectric constant of 7.6 was used to approximate THF solvation. Dynamics simulations were conducted using a 2 fs timestep, Velocity Verlet integrator and infinite van-der-Waals and Coulomb cutoff without periodic boundary conditions. Bond lengths involving hydrogen atoms were constrained using the SHAKE algorithm[25] and the system temperature was coupled to an external bath *via* a Langevin thermostat with coupling constant of 2 ps$^{-1}$.[26,27] Previous to production simulations, all molecules were subjected to a simulated annealing procedure to remove starting structure bias. The equilibration protocol included 500 steps of steepest descent minimization, followed by a 100 ps heating to 298 K. This was followed by ten repetitions of a heating/cooling cycle alternating between 100 ps MD at 450 K and 100 ps simulations cooling to 298 K. After equilibration, data collection MD simulations were run for 10 ns at 298 K. Simulations progressed at 2.5 ns/day for single CPU processes on common hardware.

The dihedral angles α and γ which define the orientation of the sec-butyl and benzyl groups, respectively, are shown in (Fig. 3). The dihedral angle β defines the tetrahydropyran ring twist. The distance d between the carboanion and its point of attack is also indicated.

Each 10 ns trajectory was divided into three clusters using the means algorithm of the ptraj module in *Amber*.[28] A representative structure is shown for each cluster in (Fig. 4) (top to bottom rows: **7′**, **10′**, **8** and **11**). Numbers below each conformation indicate the size of the conformational cluster compared to the full trajectory.

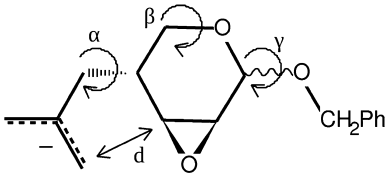


**Fig. 3.** Definition of geometrical parameters.

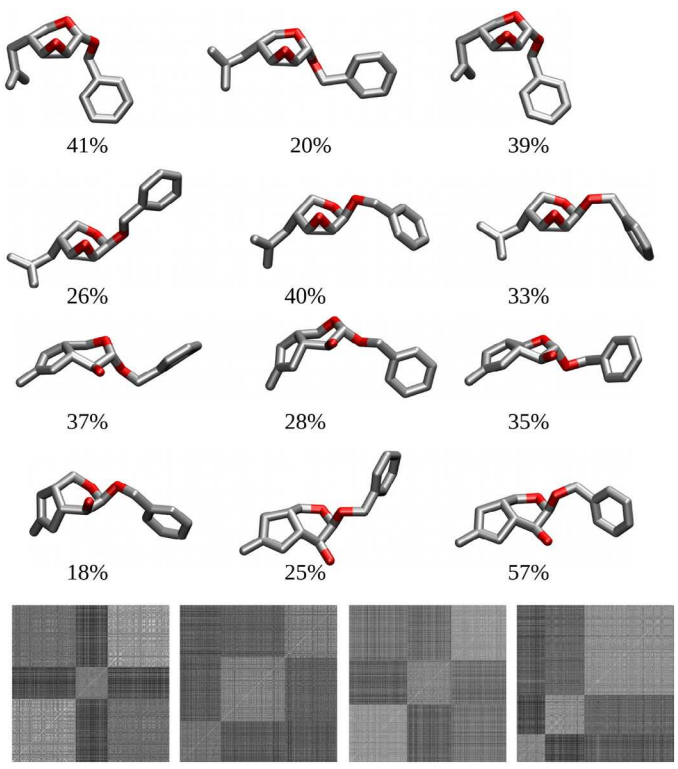


**Fig. 4.** Clustering analysis and 2D-rmsd values for all studied molecules. Hydrogen atoms are omitted for clarity.

The reaction intermediates **7′** and **10′** adopt preferably compact folded and elongated conformations, respectively. The carboanion is located closer to its point of attack in the six-membered ring in **7′** than in **10′**. For the final products **8** and **11**, the fused rings inhibit conformational flexibility and the conformational clusters differ mainly in the orientation of the benzyl chain. Below: 2D rmsd plots for the clustered trajectories give an indication of similarity between clusters (from left to right: **7′**, **10′**, **8** and **11**). Lighter colors indicate higher similarity of structures. Notably, for **7′** the cluster 2 is fairly different from clusters 1 and 3.

## Acknowledgments

The authors would like to thank The Research Council of Oman (Grant No. RC/SCI/CHEM/14/01) for financial support.

## References

1. Shimokawa K, Takamura H, Uemura D. *Tetrahedron Lett* 2007;*48*:5623–5.
2. Helmboldt H, Rehbein J, Hiersemann M. *Tetrahedron Lett* 2004;*45*:289–92.
3. Zou L-H, Philipps A, Raabe R, Enders D. *Chem Eur J* 2015;*21*:1004–8.
4. Malinowski JT, Sharpe RJ, Johnson JS. *Science* 2013;*340*:180–2.
5. Lopalco L. *Viruses* 2010;*2*:574–600.
6. Knowles JP, O'Connor VE, Whiting A. *Org Biomol Chem* 2011;*9*:1876–86.
7. Bøjstrup M, Lundt I. *Org Biomol Chem* 2005;*3*:1738–45.
8. Elsner P, Jetter P, Brödner K, Helmchen G. *Eur J Org Chem* 2008;*15*:2551–63.
9. Schmidt AW, Olpp T, Baum E, Stiffela T, Knölker H-J. *Org Biomol Chem* 2010;*8*:4562–8.
10. Kaeobamrung J, Bode JW. *Org Lett* 2009;*11*:677–80.
11. Asano M, Nakamura T, Sekiguchi Y, Mizuno Y, Yamaguchi T, Kuroda T, et al. *Tetrahedron Asymmetry* 2013;*24*:449–56.
12. Abdel-Jalil RJ, Al-Qawasmeh RA, Al-Abed Y, Voelter W. *Tetrahedron Lett* 1998;*39*:7703–4.
13. Abdel-Jalil RJ, Shah ST, Khan K, Voelter W. *Lett Org Chem* 2005;*2*:306–8.
14. Saeed M, Abbas M, Abdel-Jalil RJ, Zahid M, Voelter W. *Tetrahedron Lett* 2003;*44*:315–7.
15. Saeed M, Abdel-Jalil RJ, Voelter W, El-Abadelah M. *Chem Lett* 2001;*7*:660–1.
16. Krief A, Dumont W. *Tetrahedron Lett* 1997;*38*:657–60.
17. Abdel-Jalil RJ, Shah ST, Khan K, Voelter W. *Lett Org Chem* 2005;*2*:238–41.
18. Abdel-Jalil RJ, Saeed M, Voelter W. *Tetrahedron Lett* 2001;*42*:2435–7.
19. Walker RC, Crowley MF, Case DA. *J Comput Chem* 2008;*29*:1019–31.
20. Case DA, Darden TA, Cheatham TE, Simmerling CL, Wang J, Duke RE, et al. *AMBER 11*. San Francisco: University of California; 2010.
21. Stewart JJP. *Comput Chem* 1989;*10*:209–20.
22. Hawkins GD, Crame CJ, Truhlar DG. *J Phys Chem* 1996;*100*:19824–39.
23. Tsui V, Case DA. *Biopolymers* 2001;*56*:275–91.
24. Hawkins GD, Cramer CJ, Truhlar DG. *Chem Phys Lett* 1995;*246*:122–9.
25. Ryckaert J, Ciccotti G, Berendsen HJC. *J Comput Phys* 1977;*23*:327–41.
26. Loncharich R, Brooks B, Pastor R. *Biopolymers* 1992;*32*:523–35.
27. Brooks C, Bruenger A, Karplus M. *Biopolymers* 1985;*24*:843–65.
28. Shao J, Tanner SW, Thompson N, Cheatham TE. *J Chem Theory Comput* 2007;*3*:2312–34.